The roles of hydrophobic group on the surface of ultra low dielectric constant porous silica film during thermal treatment

Jen-Tsung Luo [a],*, Wen-Fa Wu [b], Hua-Chiang Wen [a], Ben-Zu Wan [c], Yu-Ming Chang [a], Chang-Pin Chou [a], Jun-Ming Chen [d], Wu-Nan Chen [d]

[a] Department of Mechanical Engineering, National Chiao Tung University, Hsinchu, Taiwan
[b] National Nano Device Laboratories, Hsinchu, Taiwan
[c] Department of Chemical Engineering, National Taiwan University, Taipei, Taiwan
[d] Department of Computer and Communication, SHU-TE University, Kaohsiung 824, Taiwan

Abstract

Porous silica films with ultra low-k (below 2) and low leakage current densities (10^{-8} A/cm^2 or lower at an electric field of 1.8 MV/cm) were prepared by the surfactant-template method. Hexamethyldisilazane (HMDS), a surface modification agent, was utilized to yield hydrophobic groups on the surface of porous silica film to prevent the absorption of moisture. It effectively retained the low permittivity properties of the films. Thermal treatment at high temperature (>350 °C) destroyed surface hydrophobic groups and generated hydrophilic groups (Si–OH), which replaced the surface Si(CH$_3$)$_3$ groups, and resulted in the absorption of moisture. However, Si–OH not only resulted in the absorption of moisture but also initiated the formation of trimethylsilyl groups on the surface by HMDS. When the damaged film is repaired by HMDS again, the k value falls to its initial value (which may be below 1.6). A denser hydrophobic low-k film is formed and the electrical properties are improved.
© 2007 Elsevier B.V. All rights reserved.

Keywords: HMDS; Porous silica; Dielectric constant; Thermal treatment

1. Introduction

As electronic devices are increasingly miniaturized to the deep submicron regime, the rapid increase in the resistance–capacitance (RC) time delay is becoming a major obstacle for the development of deep submicron devices [1–3]. The feasibility of using materials with ultra low dielectric constants, instead of conventional SiO$_2$, to reduce the capacitance of the interconnection and address the RC delay problem has received considerable attention [4–6]. Porous silica films with nanometer pores may be useful as materials with ultra low dielectric constants in advanced semiconductor devices. The advantage of these materials, in addition to their low dielectric constant, is that their pores are much smaller than the features of the devices [7–11]. They are deposited using conventional spin-on methods, and the precursors resemble those currently used in the microelectronic industry. An important issue in ultra large scale integration applications is the thermal stability of the porous silica films [12–15].

This study not only investigates how thermal stressing affects porous silica films, but also discusses methods for improving thermal stability. According to the report of Yanazawa [16], during thermal treatment, the affinity of porous silica for water exceeds those of SiLK®™, tetraethylorthosilicate (TEOS) and wet-oxidized SiO$_2$. It absorbs decuple times more water than general silicon dioxide, because the hydrophobicity is lower. Hydrophobic treatment of the sol–gel silica film, such as trimethylchlorosilane, tetraethylstannane, 3-aminopropyltriethoxysilane, hexabutyldistannoxane and HMDS methods has been investigated [17–22]. The HMDS modified method is reportedly the most effective method for modifying the surface in the low dielectric area, and it is also commonly employed in the semiconductor industry [23]. Not only the pore structure but also the hydrophobic characteristics are important factors in maintaining the properties of the low dielectric constant of the porous

---

silica film [24]. The surface of the hydrophobic treated sample had a large amount of trimethylsilyl. However, heating stress removed these methyl groups and caused the absorption of moisture. A second HMDS restoration made the film hydrophobic again and solved the problem of the film's thermal instability. Accordingly, this work studies the roles of hydrophobic group on the surface of a nanoporous film with an ultra low dielectric constant during thermal stressing.

2. Experiment

The sol–gel solution was prepared by combining a molecular template (polyoxyethylene sorbitan monooleate (Tween80)), deionized water, ethanol, hydrochloric acid and TEOS. The mixing ratio (by weight) of Tween80:deionized water:ethanol: hydrochloric acid:TEOS was 2.7:1:6:0.3:3.4. The mixed solution was stirred for 3 h at room temperature to yield a sol–gel solution, which was then spin-coated on silicon wafers. The film was then soft-baked at 106 °C for 1 h to solidify the pore template and form a three-dimensional net structure. Subsequently, the film was calcined at 400 °C in a furnace for 30 min to burn out the template and solidify the pore structure again. The films were then modified to be hydrophobic by immersing them in HMDS/toluene (2/1 by a weight) solution at 80 °C for 1.5 h and dried at 100 °C for 3 min.

After the porous silica films were prepared, they further received a thermal treatment in nitrogen ambient at 350–500 °C for 30 min to evaluate their thermal stability. After thermal treatment, some samples were immersed in HMDS solution again. The films were then thoroughly washed with toluene, filtered off and dried in vacuum desiccators at room temperature. Finally, the samples were heated at 200 °C for 10 min with nitrogen flow to remove residual moisture.

A metal-insulator-semiconductor (MIS) structure, presented in Fig. 1, was formed by sputtering aluminum dots onto the dielectric film to form the top electrode, which was used to measure the capacitance and leakage current. A Keithley Model 82 C-V meter was adopted to measure the capacitance of the MIS capacitor. The capacitance–voltage curves were obtained at 1 MHz with an alternating bias. Leakage current densities were measured by an hp 4145B semiconductor parameter analyzer. Fourier transform infrared spectroscopy (FTIR) was employed to elucidate the chemical structure of the film. The thickness and morphology of the films were observed using a HITACHI S-4000 scanning electron microscope and an NT-
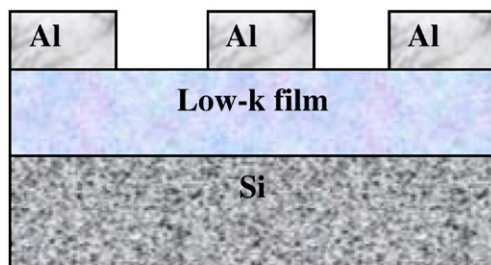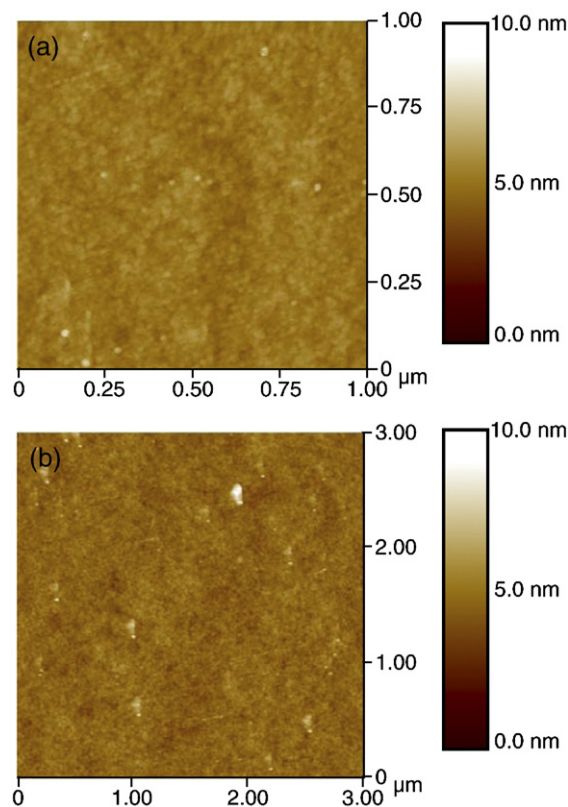

Fig. 2. AFM images of porous low-k films after (a) 500 °C annealing and (b) 500 °C annealing with HMDS restoration.

MDT Solve P47 atomic force microscope (AFM), which had a resolution of 2 nm along the x and y axes and 0.07 nm along the z axis. The scanning rate is 1.1 Hz with a 512×512-points high-resolution scanner. A thermal desorption spectrometer (TDS) was utilized to monitor the amount of moisture (H_2O) and methyl desorbed from porous silica films. The chemical composition and specific bonding characteristics were studied by angle-resolved X-ray photoelectron spectroscopy (XPS), using a VG Microlab 310F with an argon ion sputtering, performed at ion energy of 25 keV and chamber pressure of 10^{-7} Pa. XPS spectra were obtained after Ar^+ sputtering for 30 min. For the XPS analyses, films were excited with AlKα (1486.3 eV) X-rays. The reference of sensitivity factor is established by Al source. Relative to C 1s=1, the sensitivity factor of Si 2p, and O 1s are 0.82 and 2.93, respectively. The refractive index of the silica film was determined by a spectrophotometer (n&k Analyzer 1200, n&k Technology, Inc., USA).

3. Results and discussion

The topography of the samples was observed using AFM, as displayed in Fig. 2. The root mean square surface roughness of the thermally treated and HMDS restored samples was in the range from 0.34 to 0.39 nm. The surface roughness did not markedly change after thermal and HMDS restorative treatment.
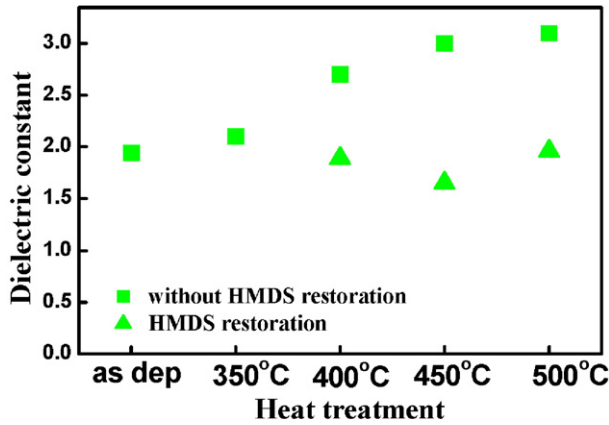

Fig. 1. Scheme of the MIS structure.

Fig. 3. Dielectric constant of the porous low-k film as a function of annealing temperature and HMDS restoration.

Fig. 5. FTIR spectra of low-k films after thermal treatments at various temperatures.

The k-value of the as-deposited film was found to be 1.97 using a MIS capacitor, according to the equation $k = Cd/\varepsilon_{o}A$ [25], where C is the capacitance of the MIS capacitor; d is the thickness of the low-k film. A is the area of the top Al electrode, and ε_{o} is the permittivity of free space. The leakage current density was 10^{-8} A/cm² at 1.8 MV/cm. Thermal stressing at 500 °C significantly increased the k value from 1.97 to 2.9 and increased the leakage current density from 10^{-8} to 10^{-5} A/cm² at 1.8 MV/cm, as shown in Figs. 3 and 4.

The low-k films retain their electrical properties after 350 °C treatment. The film is thermally stable up to about 350 °C. The dielectric constant and the leakage current increased obviously after thermal stressing at higher than 350 °C. This study considers the thermal stressing induced electrical degradation from two possible effects.

The first possible effect is that thermal stressing destroys the internal structure of the porous silica film. If pores cannot withstand high temperature stressing and are destroyed, then the total dielectric constant and the leakage current density will increase. However, some researches had reported that the structure of porous silica was thermally stable to above 900 °C [26]. FTIR spectra, shown in Fig. 5, indicate that the main
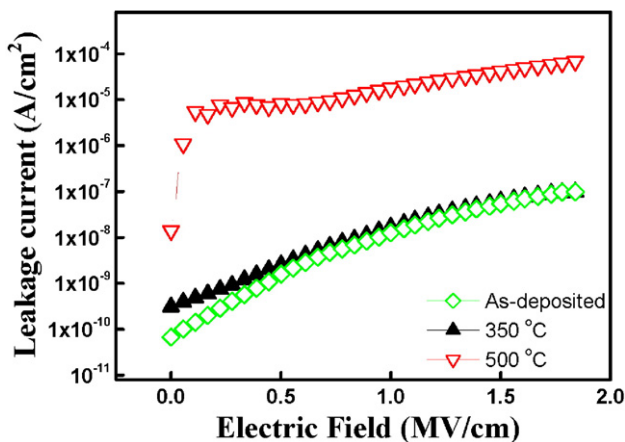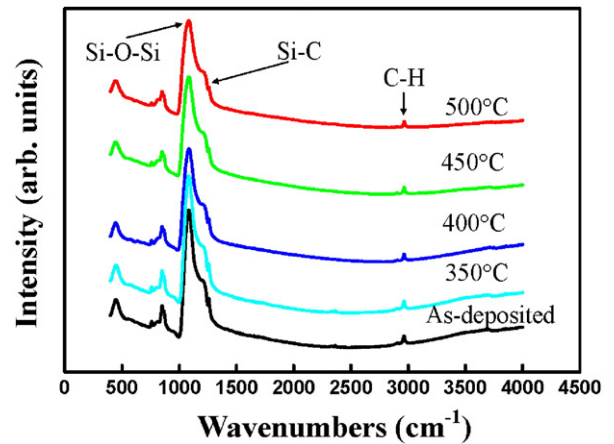
compositional structures of silica films, such as Si–O–Si and SiO₂, do not change during thermal treatment. The strong absorption peak at 1000–1200 cm⁻¹ is due to stretching vibration of Si–O–Si, in which the oxygen atom moved in the direction parallel to a line and joined the two silicon atoms. The shifting change of Si–O–Si bonding shifted toward higher wave number as temperature rose. The Si–O–Si band shifted from approximately 1076 to 1091 cm⁻¹ with $\Delta x = 15$ cm⁻¹. R. A. Orozco-Teran and G. L. Lucovsky reported that the shift was caused by the increase in the bond angle [27,28]. The shift in the Si–O peak to a higher wave number also demonstrates that organic groups evaporated and dissociated from the surface during thermal treatment and some new groups, such as silanols, were grafted. The peaks at 1260 cm⁻¹ and 3050 cm⁻¹ are attributable to the Si–C and the symmetric vibration of C–H bonds. The peak at 760–860 cm⁻¹ is associated with the stretching vibration of methyl species within the trimethylsilyl groups [29,30]. The peak intensity slightly decreased upon thermal treatment at over 400 °C. However, after thermal treatment at 350–500 °C, the main peak of Si–O–Si is almost the same as that of as-deposited one.

The porosity of the films can be determined from the refractive index according to the Lorentz–Lorenz relationship [31].

$$(n_{f}^2 - 1)/(n_{f}^2 + 2) = (1 - V_{f})(n_{s}^2 - 1)(n_{s}^2 + 2)$$

Where V_{f} is the pore volume fraction of the film; n_{f} is the measured refractive index of the porous silica film, and n_{s} is the silica skeletal refractive index of TEOS, which was taken to be

Fig. 4. Leakage current densities of low-k films after thermal treatments at various temperatures.

Table 1
Refractive index and porosity of different thermal treatments at various temperatures

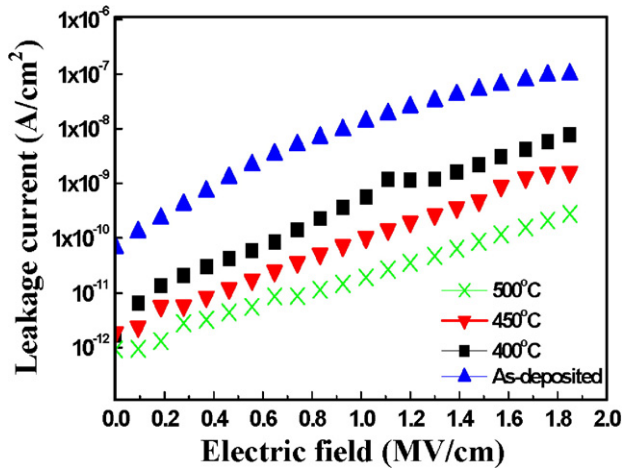| Samples	Refractive index (n)	Porosity (%)
as-deposited	1.23	47
350 °C	1.22	49
400 °C	1.23	47
500 °C	1.20	51

Fig. 6. Leakage current densities of low-k films after thermal treatments at various temperatures and HMDS restoration.

Fig. 8. TDS spectra of H2O ($m/e=18$) desorption for low-k films.

1.46. Based on the results of Table 1, the porosity did not change very much and was consistent with FTIR measurement. A high temperature neither destroyed the pore structure nor reduced the porosity. In the preparation of the low-k film, a calcination temperature of 400 °C was adopted (see experiment) before HMDS modification. The k value of the thermal calcined sample reached 1.9 after HMDS modification. Therefore, the pore structure of the low-k film is believed to be retained after thermal treatment at 400 °C.

The second possible effect is the damage of the hydrophobic groups formed by HMDS. HMDS ($((Si(CH_3)_3)_2)NH$) can form trimethylsilyl groups to replace the silanol groups and enhance the hydrophobic characteristics, which protect the film from moisture. The bonding energy of methyl (CH_3) and Si were not sufficiently high to prevent thermal damage. Hence, during thermal treatments at over 400 °C, methyl was released from the surface of the film. Finally, Si combined with the O–H groups, such that moisture was absorbed easily and the k-value increased.

The samples were again treated by HMDS to show that the poor thermal stability was caused by the destruction of trimethylsilyl groups. The results indicated that the k value decreased from 3 to ~1.8, as indicated by the triangular

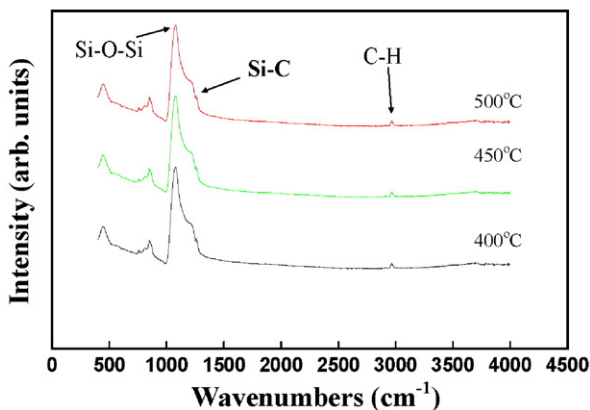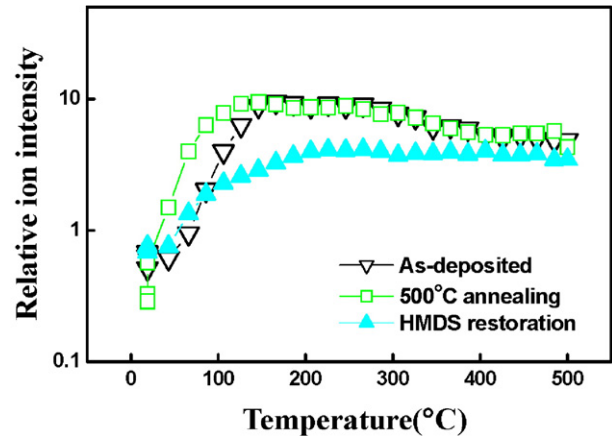symbols in Fig. 3, and the leakage current density fell from 10^{-4} to ~10^{-11} A/cm^2 at 1.8 MV/cm, as presented in Fig. 6. The improvement in electrical performance is obvious. The annealed sample at 500 °C had the largest leakage current density. The electrical properties of the samples following HMDS restoration are better than that of the as-deposited one. The poor thermal stability of a porous silica film followed the breaking of the chemical bonds between Si and methyl by high-temperature stressing. Fig. 7 showed the FTIR spectra of thermally stressed films at temperatures from 400 to 500 °C and those that had undergone HMDS restoration. The 3740 cm^{-1} peak was associated with isolated silanols (SiO–H) and this peak was relieved by HMDS restoration. The peak intensity of CH_x and Si–C also increased slightly.

After thermal treatment and HMDS restoration, the dielectric constant was lower than that of the as-deposited film. Fig. 8 shows the TDS spectra of H$_2$O ($m/e=18$) desorption for low-k films. Moisture will be desorbed from the film at high temperatures. Before 100 °C, the relative intensity increased rapidly. The curve gradient increased slowly as the temperature exceeds 100 °C. The second possible effect refers to damage of the hydrophobic groups formed by HMDS. The line of upper triangular symbols referred to the 500 °C-annealed sample following HMDS restoration. The amount of moisture desorbed from the surface is lower than that of

Fig. 7. FTIR spectra of low-k films after thermal treatments at various temperatures and HMDS restoration.

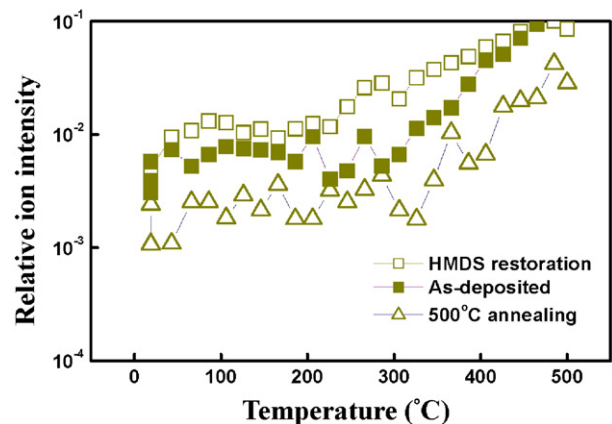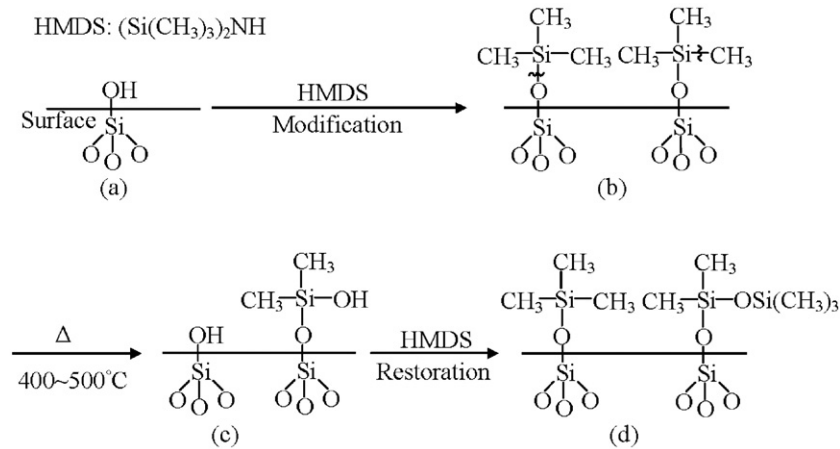Fig. 9. TDS spectra of CH3 ($m/e=15$) desorption for low-k films.

Fig. 10. Schematic representation of (a) surface silanol groups, (b) surface modification, (c) thermal treatment, and (d) surface hydrophobic restoration.

the other samples, indicating that the surface chemical groups of the samples with HMDS restoration are hydrophobic and moisture is not easily absorbed on whose surface. The TDS spectra of H_2O desorption indicate that samples without HMDS restoration have the highest moisture absorption. The samples with HMDS restoration ease the absorption of moisture.

Fig. 9 shows the TDS spectra of methyl ($m/e = 15$) desorbed from low-k films. Methyl is a nonpolar group because the electro-negativity between C and H atoms is very small. Methyl is important in preventing the absorption of water, which has a polar bond between O and H because the electro-negativity between O and H atoms is very large. An impulse is applied between the polar and nonpolar bond, subsequently dividing them. The sample annealed at 500 °C had the least methyl, while that re-treated with HMDS had the most. From Fig. 9, the amount of methyl desorption clearly increased with temperature from 300 °C which was lower than the thermal stability of 350 °C. The dielectric constant increased with temperature over 350 °C. The decline in the amount of methyl increased k value.

The structure of porous silica films includes Si–OH groups as well as traditional $(SiO_2)_x$. Si–OH groups can easily combine with moisture. The adsorption of H_2O with a dielectric constant of 78 onto the film's surface increases the dielectric constant of the film. Based on the aforementioned results, Fig. 10 presents a mechanism involved in surface modification, thermal stressing and HMDS restoration [32–34]. Fig. 10a shows the surface silanol group without hydrophobic treatment. Following HMDS modification, the H atom of Si–OH reacted with the amino group (=NH) of HMDS to yield NH_3 and the silanol group was replaced by trimethylsilyl of HMDS to promote hydrophobic properties, as displayed in Fig. 10b. The samples were tested by thermal treatment. In a high-temperature ambience, the film was attacked by oxygen radicals to generate a large amount of surface –OH groups. E. Kondoh [35] reported that oxygen radicals diffused into the nanopores of the surface and reacted with –H or replaced organic groups, such as CH_3, that are bonded to the Si atoms of the Si–O bonds. Finally, –OH groups or Si–OH groups were formed. The bond dislocation energy of Si–O is 798 kJ/mol and that of Si–C is 435 kJ/mol. Hence, the

Si–C bond is assumed to be more easily broken by high temperature than the Si–O bond. Therefore, the SiOSi $(CH_3)_2OH$ yield exceeded the SiOH yield, as presented in Fig. 10c, in which hydroxyl groups are attached to the $\equiv SiCH_3$ surface, resulting in a significant amount of water. The absorption of –OH not only attracted moisture but also initiated the modification of the surface by HMDS again. Fig. 10d shows the possible HMDS restoration reaction in which the $Si(CH_3)_3$ group is grafted onto the $SiOSi(CH_3)_2$–OH or the Si–OH surface to yield $SiOSi(CH_3)_2OSi(CH_3)_3$ or $SiOSi(CH_3)_3$ group. The thermally treated and HMDS-restored samples have better electrical characteristics than the as-deposited ones. During an IC fabrication process, the low dielectric constant film will suffer the absorption of moisture or high temperature and the increase of dielectric constant is unavoidable. Hydrophobic restoration can be the last procedure in the process, to ensure that the low-k material is hydrophobic, and the electrical properties are maintained.

Table 2 presents the compositions of the samples identified by XPS. C is believed to be resulted from the Si-methyl groups. The 500 °C-heated sample had the lowest C/Si ratio, and the drop in C content may be caused by the heat treatment. The O is in the O–H and Si–O groups. Si–O groups are major components of porous silica films. The as-deposited sample had the largest O/Si ratio, of around two, which approximates the atomic ratio of SiO_2. The sample with HMDS restoration had the lowest O/Si ratio, because HMDS restoration increased the amount of Si at the surface.

Table 2
Compositions of porous silica films analyzed by XPS

	Percentage (%)			Composition ratio	
	O (%)	C (%)	Si (%)	O/Si	C/Si
as-deposited	56	17	27	2.1	0.64
500 °C-annealed	59	9	32	1.9	0.27
500 °C-annealed+HMDS restoration	53	14	33	1.6	0.41

4. Conclusion

Porous low-*k* films with an ultra-low dielectric constant below 2 and a breakdown field more than 2 MV/cm were prepared by a templating method. Thermal stress at temperatures exceeding 350 °C clearly degraded the electrical properties, because the surface was hydrophilic. However, the hydrophilic properties were recovered by a second HMDS restoration. FTIR, TDS and XPS analyses demonstrate that after a second HMDS restoration, the silanol group on the thermally damaged surface was replaced again by a methyl group. High temperature broke the Si–C bond and silanol groups were formed. The existence of Si–OH group enabled trimethylsilyl groups of HMDS to graft on the surface again and made the surface more hydrophobic. A recovery of electrical properties of porous silica film was obtained after HMDS restoration.

References

[1] M.T. Bohr, Proceedings of International Electron Devices Meeting, IEEE, Washington, DC, 1995, p. 241.
[2] R. Wilson, C.T. Tracy, T.L. Freeman, Handbook of Multilevel Metallization for Integrated Circuits: Materials, Technology and Application, Noyes Publications, Park Ridge, USA, 1993.
[3] S. Mizuno, A. Verma, H. Tran, P. Lee, B. Nguyen, Thin Solid Films 283 (1996) 30.
[4] V. Ligatchev, T.K.S. Wong, B. Liu, Rusli, J. Appl. Phys. 92 (2002) 4605.
[5] C.Y. Ting, D.F. Ouan, B.Z. Wan, J. Electrochem. Soc. 150 (2003) F164.
[6] T.G. Tsai, A.T. Cho, C.M. Yang, F.M. Pan, K.J. Chao, J. Electrochem. Soc. 149 (2002) F116.
[7] J.Y. Kim, M.S. Hwang, Y.H. Kim, H.J. Kim, Y. Lee, J. Appl. Phys. 90 (2001) 2469.
[8] H.J. Lee, C.L. Soles, D.W. Liu, B.J. Bauer, E.K. Lin, J. Appl. Phys. 95 (2004) 2355.
[9] L. Sandrin, M.S. Silverstein, E. Sacher, Polymer 42 (2001) 3761.
[10] D.G. Shamiryan, M.R. Baklanov, S. Vanhaelemeersch, K. Maex, Electrochem. Solid-State Lett. 4 (2001) F3.
[11] C.J. Brinker, G.W. Scherer, Sol–Gel Science, Academic Press, San Diego, 1990.
[12] M.H. Jo, H.H. Park, D.J. Kim, S.H. Hyun, S.Y. Choi, J.T. Paik, J. Appl. Phys. 82 (1997) 1299.
[13] J.N. Sun, D.W. Gidley, T.L. Dull, W.E. Frieze, A.F. Yee, E.T. Ryan, S. Lin, J. Wetzel, J. Appl. Phys. 89 (2001) 5138.
[14] H. Miyajima, R. Katsumata, Y. Nishiyama, Jpn. J. Appl. Phys. 35 (1996) 6217.
[15] Y.L. Cheng, Y.L. Wang, J.K. Lan, G.J. Hwang, M.L. O'Neil, C.F. Chen, Surf. Coat. Technol. 200 (2006) 3127.
[16] H. Yanazawa, T. Fukuda, Y. Uchida, I. Katou, Surf. Sci. 566–568 (2004) 566.
[17] G. Akovali, Z.M.O. Rzaev, D.H. Mamedov, J. Appl. Polym. Sci. 58 (1995) 645.
[18] S.K. Singh, A.A. Kumbhar, R.O. Dusane, Mater. Sci. Eng., B, Solid-State Mater. Adv. Technol. 127 (2006) 29.
[19] Y.S. Mor, T.C. Chang, P.T. Liu, T.M. Tsai, C.W. Chen, S.T. Yan, C.J. Chu, W.F. Wu, F.M. Pan, W. Lur, S.M. Sze, J. Vac. Sci. Technol., B 20 (2002) 1334.
[20] C.C. Cho, B.E. Gnade, D.M. Smith, U.S. Patent No. 5504042, 2 Apr. 1996.
[21] S.V. Nitta, V. Pisupatti, A. Jain, P.C. Wayner, W.N. Gill, J.L. Plawsky, J. Vac. Sci. Technol., B 17 (1999) 205.
[22] X.S. Zhao, G.Q. Lu, J. Phys. Chem., B 102 (1998) 1556.
[23] P. Bankovic, Mater. Sci. Eng., B, Solid-State Mater. Adv. Technol. 112 (2004) 165.
[24] B.P. Gorman, R.A. Orozco-Teran, Z. Zhang, P.D. Matz, D.W. Mueller, R.F. Reidy, J. Vac. Sci. Technol., B 22 (2004) 1210.
[25] C. Kittel, Introduction to the Solid State Physics, 6 ed. Wiley, New York, 1986.
[26] T. Furusawa, D. Ryuzaki, R. Yoneyama, Y. Homma, K. Hinode, J. Electrochem. Soc. 148 (2001) F175.
[27] R.A. Orozco-Teran, B.P. Gorman, D.W. Mueller, M.R. Baklanov, R.F. Reidy, Thin Solid Films 471 (2005) 145.
[28] G.L. Lucovsky, M.J. Manitini, J.K. Srivastava, E.A. Irene, J. Vac. Sci. Technol., B 5 (1987) 530.
[29] A.L. Smith, The Analytical Chemistry of Silicones, Wiley, New York, 1991, p. 307.
[30] A.L. Smith, Spectrochim. Acta 16 (1960) 87.
[31] M. Born, E. Wolf, Principles of Optics, Pergamon Press, New York, 1983, p. 87.
[32] T.I. Suratwala, M.L. Hanna, E.L. Miller, P.K. Whitman, I.M. Thomas, P.R. Ehrmann, R.S. Maxwell, A.K. Burnham, J. Non-Cryst. Solids 316 (2003) 349.
[33] S. Yu, X. Hu, V. Ligatchev, J. Appl. Phys 92 (2002) 3338.
[34] T.C. Chang, P.T. Liu, Y.S. Mor, S.M. Sze, J. Vac. Sci. Technol., B 20 (2002) 1561.
[35] E. Kondoh, T. Asano, A. Nakashima, M. Komatu, J. Vac. Sci. Technol., B 18 (2000) 1276.